Journal of Sound and Vibration (2001) **242**(4), 681–699
doi:10.1006/jsvi.2000.3385, available online at http://www.idealibrary.com on IDEAL®

VIBRATION SUPPRESSION IN ROTATING BEAMS USING ACTIVE MODAL CONTROL

Y. A. KHULIEF

Department of Mechanical Engineering, King Fahd University of Petroleum & Minerals, KFUPM Box 1767, *Dhahran* 31261, *Saudi Arabia. E-mail: khulief@kfupm.edu.sa*

(*Received* 22 *December* 1999, *and in final form* 6 *September* 2000)

Advances in technology and the underlying demand for achieving high performance has resulted in a class of light-weight high-speed mechanical systems. Light-weight mechanical components are prone to appreciable elastic deformations and experience vibrational motions. Vibration suppression in rotating elastic members is of major importance in many engineering applications. Examples are robot manipulators, propellers, turbomachines, high-speed flexible mechanisms, and space deployable systems. Active control falls among the most feasible techniques for vibration suppression in rotating structures, where passive techniques may become ineffective or impractical. The vibrational motion of the rotating elastic member is represented by a finite element dynamic model, which is written in terms of a reduced set of modal co-ordinates. A realistic set of modal co-ordinates that accounts for the dynamically induced stiffening effect due to reference rotation is introduced. Pointwise observation and control are employed in association with an optimal state-variable feedback strategy. The control scheme developed is applied to a rotating beam, and the dynamic responses of both the controlled and residual frequency subsystems are numerically evaluated.

1. INTRODUCTION

Semi-active controllers utilizing the technique of activated damping have been implemented in several vibration suppression applications [1–3]. The prescribed control law, in this case, is based on remote sensing of structural deflections and velocities, as well as deflections and velocities at the attachment point. Consequently, the control action is devoted to adjusting the existing damping mechanism.

Active controllers have been developed and implemented in sound attenuation and room reverberation for many years [4, 5]. However, active control of vibrations is relatively less well developed, simply because of the complex deformations of structures. Unlike activated dampers, active controllers are capable of sensing remote velocities and deflections, and producing certain control commands that feed a set of force generators attached to some selected locations. Active controllers have the advantage of operating over a wide-frequency range, creating an equivalent electronic gain for mass, and achieving good performance at the low-frequency range. The latest is of great importance in controlling plate vibrations.

The early investigations by Balas [6, 7] and Meirovitch *et al.* [8] have laid the foundation for establishing a fully active control scheme for vibration suppression in flexible structural systems. In their work, the state variable feedback, modal control, and optimal control techniques were utilized within the framework of the active controller. Moreover, the issues of controlling a reduced order model, and the consequent effect of the residual frequency subsystem were also addressed in references [6–8].

0022-460X/01/190681 + 19 $35.00/0

Some experimental investigations on active suppression of vibrations in small structures using piezoelectric actuators have been reported [9–11]. Some relatively larger scale experiments have been conducted using electromagnetic actuators [12, 13]. Different control strategies were invoked by the reported experimental studies, which included simple velocity feedback, simple adaptive feedforward techniques, and modal feedback control using a set of spectral filters. Other analytical studies of active vibration control in elastic beams have been reported [14–16].

The previously cited mathematical models are developed for non-rotating elastic structures, and have not utilized the powerful finite element method. Although, the use of finite element was recognized at the early stage [7, 8], only very few studies can be cited in the literature [3, 13], wherein the finite element method is employed in conjunction with semi-active control schemes.

Active control of rotating shafts has been addressed through active damping and magnetic bearing techniques, see e.g., references [17, 18]. Application of active control techniques to rotating structures, in general, are much less represented in the available literature. Although, several investigations have addressed the problem of vibration control of an elastic manipulator link [19–21], they based their controller design on elastodynamic models of a non-rotating elastic beam.

In this paper, the analytical design of an active control scheme for vibration suppression in an elastic rotating beam has been addressed. The elastic beam is modelled by using the consistent finite element approach, and the elastodynamic model of the rotating beam is formulated in the state space. The control strategy is based on optimal modal control of a set of significant modes, while state estimation for the deterministic case is also employed. The state estimator has the elastodynamic equations of a rotating beam as its internal model. Consequently, the effect of beam rotation is carried over into the solution of the optimal regulator problem. The developed computational algorithm is applied to a rotating beam, where different controller designs are considered, and the effect of the rate of spin on the controller performance is numerically evaluated. In addition, the effect of material damping on the residual vibrational modes has also been addressed.

2. THE FINITE ELEMENT MODEL

2.1. KINETIC ENERGY EXPRESSIONS

The finite element method provides the most powerful modelling technique for elastic structures, with the potential capability of handling complex structural configurations. Therefore, the finite element method will be utilized in deriving the elastodynamic equations.

The rotating elastic beam can be discretized into a set of finite beam elements. Three systems of co-ordinates are employed to describe the global position of any arbitrary point on the beam. These are, the inertial reference frame XYZ, the rotating beam reference axes xyz, and the ith element axes $x^i y^i z^i$, as shown in Figure 1. Now, the global position $\{r_p^i\}$ of an arbitrary point p^i can be expressed as

$$\{r_p^i\} = [R][N^i]\{e^i\}, \tag{1}$$

where $[R(\theta)]$ is the co-ordinate transformation matrix, $[N^i]$ is a modified elemental shape function that accounts for a transformation from the element co-ordinates to the beam

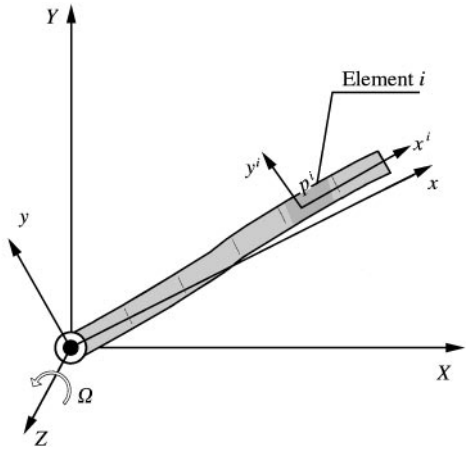

Figure 1. The elastic beam co-ordinate system.

co-ordinate system, and $\{e^i\}$ is the vector of element nodal co-ordinates. Here, the elastic deformations are confined to the plane of rotation. Differentiating equation (1) with respect to time, one obtains the global velocity vector as

$$\{\dot{r}_p^i\} = [[H^i] \quad [R]\,[N^i]] \begin{Bmatrix} \{\dot{\theta}\} \\ \{\dot{e}^i\} \end{Bmatrix}, \tag{2}$$

where $[H^i]\{\dot{\theta}\}$ represents the expression $[\dot{R}][N^i]\{e^i\}$, which results from differentiating the right-hand side of equation (1) with respect to time. Now, one can write the kinetic energy expression of the ith element as

$$T^i = \frac{1}{2}\int_{V^i} \rho^i \begin{Bmatrix} \{\dot{\theta}^i\} \\ \{\dot{e}^i\} \end{Bmatrix}^{\mathrm{T}} \begin{bmatrix} [H^i]^{\mathrm{T}}[H^i] & [H^i]^{\mathrm{T}}[R][N^i] \\ [N^i]^{\mathrm{T}}[R]^{\mathrm{T}}[H^i] & [N^i]^{\mathrm{T}}[N^i] \end{bmatrix} \begin{Bmatrix} \{\dot{\theta}^i\} \\ \{\dot{e}^i\} \end{Bmatrix} \mathrm{d}V^i. \tag{3}$$

The integrals of equation (3) can be reduced to the following forms:

$$\int_{V^i} \rho^i [H^i]^{\mathrm{T}}[H^i]\,\mathrm{d}V^i = \{e^i\}^{\mathrm{T}} \int_{V^i} \rho^i [N^i]^{\mathrm{T}}[N^i]\,\mathrm{d}V^i \{e^i\} = \{e^i\}^{\mathrm{T}}[M^i]\{e^i\}, \tag{4}$$

$$\int_{V^i} \rho^i [H^i]^{\mathrm{T}}[R][N^i]\,\mathrm{d}V^i = \{e^i\}^{\mathrm{T}} \int_{V^i} \rho^i [N^i]^{\mathrm{T}}[S^i][N^i]\,\mathrm{d}V^i = \{e^i\}^{\mathrm{T}}[\tilde{S}^i]. \tag{5}$$

Here $[S^i] = [R_\theta]^{\mathrm{T}}[R]$, $[R_\theta] = \mathrm{d}[R]/\mathrm{d}\theta$, and $[\tilde{S}^i]$ is a skew symmetric matrix [3]. The matrix $[M^i]$ is the conventional finite element mass matrix of the structural dynamics formulation. The mass matrix of the rotating finite element, as expressed in equation (3), can be written in the form

$$[\bar{M}^i] = \begin{bmatrix} \{e^i\}^{\mathrm{T}}[M^i]\{e^i\} & \{e^i\}^{\mathrm{T}}[\tilde{S}^i] \\ [\tilde{S}^i]^{\mathrm{T}}\{e^i\} & [M^i] \end{bmatrix}. \tag{6}$$

2.2. STRAIN ENERGY EXPRESSIONS

The local co-ordinate vector of point p^i with respect to the local element axes $x^i y^i z^i$ can be expressed as

$$\{u^i \; w^i\}^{\mathrm{T}} = [\bar{N}^i]\{e^i\}, \tag{7}$$

where the deformations are confined to the plane of rotation, and the beam is assumed to rotate about a fixed axis in space. The matrix $[\bar{N}^i]$ contains shape function defined with respect to the element co-ordinate system. Upon neglecting shear deformations, the strain energy expression may be written as

$$U^i = \frac{1}{2}\int_0^{l_i} \left\{ E^i a^i \left(\frac{\partial u^i}{\partial x^i}\right)^2 + E^i I^i \left(\frac{\partial^2 w^i}{\partial x^{i2}}\right)^2 + E^i a^i \left(\frac{\partial u^i}{\partial x^i}\right)\left(\frac{\partial w^i}{\partial x^i}\right)^2 \right\} \mathrm{d}x, \tag{8}$$

where E^i, I^i and a^i are the Young's modulus, the cross-sectional moment of inertia and the cross-sectional area of element i respectively. The first two integrals of equation (8) represent linear strain energy, while the third term is a contribution of the non-linear component of strain [22]. Equation (8) can be written in quadratic matrix form as

$$U^i = \begin{Bmatrix} \{\dot{\theta}\} \\ \{\dot{e}^i\} \end{Bmatrix}^{\mathrm{T}} \begin{bmatrix} [0] & [0] \\ [0] & [K_e^i] \end{bmatrix} \begin{Bmatrix} \{\dot{\theta}\} \\ \{\dot{e}^i\} \end{Bmatrix}, \tag{9}$$

where $[K_e^i]$ is given by

$$[K_e^i] = [K_l^i] + [K_r^i]. \tag{10}$$

The matrix $[K_l^i]$ represents the linear elastic stiffness of element i, and the matrix $[K_r^i]$ is the result of integrating the third term of equation (8), where the term $E^i a^i (\partial u^i / \partial x^i)$ accounts for the axial stresses resulting from the centrifugal force field due to spinning. The details of the non-zero entries of the matrix $[K_r^i]$ are given in reference [23].

2.3. THE ELASTODYNAMIC MODEL OF THE BEAM

The Lagrangian form of the equations of motion is obtained by performing the proper differentiations of the Lagrangian function energy expressions. The equations of motion of the flexible rotating beam can be obtained by employing the standard finite element sequential assembly procedure according to node numbering on the beam, and can be written in matrix form as

$$\begin{bmatrix} \{e\}^{\mathrm{T}}[M\{e\} & \{e\}^{\mathrm{T}}[\tilde{S}] \\ [\tilde{S}]^{\mathrm{T}}\{e\} & [M] \end{bmatrix} \begin{Bmatrix} \{\ddot{\theta}\} \\ \{\ddot{e}\} \end{Bmatrix} + \begin{bmatrix} [0] & [0] \\ [0] & [K_e] \end{bmatrix} \begin{Bmatrix} \{\theta\} \\ \{e\} \end{Bmatrix}$$

$$= \begin{Bmatrix} -2\dot{\theta}\{e\}^{\mathrm{T}}[M]\{e\} & -\{e\}^{\mathrm{T}}[\tilde{S}]\{e\} \\ \dot{\theta}[M]\{e\} & -2\dot{\theta}[\tilde{S}]^{\mathrm{T}}\{\dot{e}\} \end{Bmatrix} + \begin{Bmatrix} \{Q_\theta\} \\ \{Q_e\} \end{Bmatrix}, \tag{11}$$

where $[M]$, $[K_e]$ and $[\tilde{S}]$ are the assembled forms of the elemental matrices $[M^i]$, $[K_e^i]$ and $[\tilde{S}^i]$ respectively. The displacement vector $\{e\}$ represents all the nodal co-ordinates of the beam, while $\{Q_\theta\}$ and $\{Q_e\}$ are the generalized external forces. If the beam is rotating at

a constant angular velocity, then the vibrational motion associated with the dynamic model of equation (11) can be expressed as

$$[M]\{\ddot{e}\} + 2\dot{\theta}[\tilde{S}]^{\mathrm{T}}\{\dot{e}\} + ([K_e] - \dot{\theta}^2[M])\{e\} = \{Q_e\}, \tag{12}$$

where $\{Q_e\}$ is the vector of external nodal forces that may include the control forces. If material damping is included, then equation (12) can be written as

$$[M]\{\ddot{e}\} + [D]\{\dot{e}\} + [K]\{e\} = \{Q_e\}, \tag{13}$$

where $[D] = 2\dot{\theta}[\tilde{S}]^{\mathrm{T}} + [D_e]$, $[K] = ([K_e] - \dot{\theta}^2[M])$ and $[D_e]$ is the material damping matrix. With regard to material damping, linear and non-linear models that include both viscous and hysteretic forms of internal damping have been reported in the literature [23]. Nevertheless, linear damping models, e.g., viscoelastic Kelvin–Voigt models, have also been adopted [24]. Accurate modelling of material damping remains an issue of continued investigations [25]. For simplicity, the concept of proportional damping is adopted to utilize the practical approach of introducing modal damping. In this case, the damping matrix $[D_e]$ is assumed to be proportional to the mass matrix. However, any other material damping model can be treated similarly.

2.4. THE REDUCED MODAL FORM

The discretization of elastic systems when using the finite element method often results in a large number of nodal co-ordinates. The resulting dynamic model with a potentially very large number of degrees of freedom is, in essence, a mathematical model with a widely spread eigenspectrum. Such numerical systems are prone to numerical integration difficulties, and therefore tend to inhibit the efficiency of the finite element method in modelling large-scale structural systems. To alleviate this problem, modal reductions have been introduced [27–30]. The reduced order modal form of the equations of motion is obtained by invoking a modal transformation from the nodal space to the space of modal co-ordinates.

For the general case when the gyroscopic effect is included, one can write the eigenvalue problem in the form

$$[A_e]\{\dot{y}_e\} + [B_e]\{y_e\} = \{Q\}, \tag{14}$$

where $\{Q\} = [\{0\}^{\mathrm{T}}\ \{Q_e\}^{\mathrm{T}}]^{\mathrm{T}}$ is the generalized force vector and $\{y_e\} = [\{\dot{e}\}^{\mathrm{T}}\ \{e\}^{\mathrm{T}}]^{\mathrm{T}}$ is the nodal state vector. Now, the eigenvalue problem is solved for the two adjoint equations

$$[A_e]\{\dot{y}_e\} + [B_e]\{y_e\} = \{0\}, \qquad [A_e]^{\mathrm{T}}\{\dot{y}'_e\} + [B_e]^{\mathrm{T}}\{y'_e\} = \{0\}. \tag{15, 16}$$

Let $[\Phi_R]$ and $[\Phi_L]$ denote the complex modal matrices of the differential operators of equations (15) and (16) respeively: i.e.,

$$(\lambda_k[A_e] + [B_e])\{\Phi_R^k\} = 0, \qquad (\lambda_k[A_e]^{\mathrm{T}} + [B_e]^{\mathrm{T}})\{\Phi_L^k\}] = \{0\}, \tag{17, 18}$$

in which λ_k denotes the kth eigenvalue associated with right- and left-hand eigenvectors $\{\Phi_R^k\}$ and $\{\Phi_L^k\}$ respectively. It is noteworthy to mention that if the matrices $[A_e]$ and $[B_e]$ are symmetric, the eigenvectors $\{\Phi_R^{i^k}\}$ and $\{\Phi_L^{i^k}\}$ are equal; otherwise $\{\Phi_R^k\}$ and $\{\Phi_L^k\}$ are distinct.

Having obtained the eigenvalue problem in the state-space form, one can proceed with the important step of reducing the size of the finite element model by utilizing modal co-ordinates. Accordingly, the following modal transformation is introduced:

$$\{y_e\} = [\Phi_R]\{u\}. \tag{19}$$

Here $\{u\} = [\{\dot{u}_e\}^{\mathrm{T}}\ \{u_e\}^{\mathrm{T}}]^{\mathrm{T}}$ is the state vector in the modal space, which is composed of modal velocities and modal co-ordinates. Equation (14) can be written in an alternative state-space form as

$$\{\dot{y}_e\} = [\bar{A}]\{y_e\} + [\bar{B}]\{Q\}, \tag{20}$$

where

$$[\bar{A}] = -[A_e]^{-1}[B_e] = \begin{bmatrix} [0] & -[M] \\ [M] & [D] \end{bmatrix}^{-1} \begin{bmatrix} [M] & [0] \\ [0] & [K] \end{bmatrix}$$

$$= \begin{bmatrix} -[M]^{-1}[D]^{\mathrm{T}} & -[M]^{-1}[K] \\ [I] & [0] \end{bmatrix}, \tag{21}$$

$$[\bar{B}] = [A_e]^{-1} = \begin{bmatrix} [0] & -[M] \\ [M] & [D] \end{bmatrix}^{-1} = \begin{bmatrix} [M]^{-1}[D]^{\mathrm{T}}[M]^{-1} & [M]^{-1} \\ -[M]^{-1} & [0] \end{bmatrix}. \tag{22}$$

Now, equation (20) can be written in the transformed modal form as

$$[\Phi_R]\{\dot{u}\} = [\bar{A}][\Phi_R]\{u\} + [\bar{B}]\{Q\}. \tag{23}$$

Post-multiplying both sides by $[\Phi_L]^{\mathrm{T}}$, one obtains

$$[\Phi_L]^{\mathrm{T}}[\Phi_R]\{\dot{u}\} = [\Phi_L]^{\mathrm{T}}[\bar{A}][\Phi_R]\{u\} + [\Phi_L]^{\mathrm{T}}[\bar{B}]\{Q\}. \tag{24}$$

The square matrix $[\Phi_L]^{\mathrm{T}}[\Phi_R]$ is invertible based on the fact that all of the columns of the transformation matrix of a linear elastic structure are linearly independent. If one designates $[\Gamma] = [[\Phi_L]^{\mathrm{T}}[\Phi_R]]^{-1}$, equation (27) can be written in the form

$$\{\dot{u}\} = [\Gamma][\Phi_L]^{\mathrm{T}}[\bar{A}][\Phi_R]\{u\} + [\Gamma][\Phi_L]^{\mathrm{T}}[\bar{B}]\{Q\} = [\bar{A}]\{u\} + [B]\{Q\}, \tag{25}$$

where $[A] = [\Gamma][\Phi_L]^{\mathrm{T}}[\bar{A}][\Phi_R]$ and $[B] = [\Gamma][\Phi_L]^{\mathrm{T}}[\bar{B}]$ are the reduced order coefficient matrices. In the case of modal damping (proportional damping) and in the absence of Coriolis terms, the left and right transformation matrices $[\Phi_L]$ and $[\Phi_R]$ respectively are equal. In this case, the matrix $[\bar{A}]$ can be put in a symmetric form, thus leading to a diagonal form of $[A]$.

If other external damping mechanisms are part of the structural system, e.g., bearing damping, suspension damping, etc., then the modal characteristics may be obtained for the adjoint equation including the damping term. In such a case, one may resort to methods for modifying the mass matrix in order to account for the damping and/or gyroscopic effects [31], thus, avoiding the need to deal with a complex eigenvalue problem. The results reported in reference [32] show that, even for systems with gyroscopic and external damping, the reduced order model using planar modes is of sufficiently high accuracy when compared to the one obtained by using complex modal reduction. Equation (25) can be written in the state-space form

$$\{\dot{u}\}_{(2mx1)} = [A]\{u\} + [B]\{Q\} \tag{26}$$

and the measurement vector as

$$\{v\}_{(2lx1)} = [C]\{u\}, \tag{27}$$

where m is the number of modes included in the model. The observation matrix $[C] = [[0]\,[\bar{C}]]$, where $[\bar{C}]$ represents entries of the observation matrix associated with displacements. At this stage, one needs to state that observations are carried out by obtaining response measurements using l sensors located at a specified set of structural nodal points. The sensor locations are to be properly chosen to satisfy the observability requirement for the controlled modes [4, 7].

2.5. SIGNIFICANT AND RESIDUAL FREQUENCY SUBSYSTEMS

If the actual plant dynamics is represented by a large number—of deformation modes, one may wish to control only a subset of significant vibration modes. The rest of the vibration modes will be considered as a residual or uncontrolled subsystem. Accordingly, the modal co-ordinate vector $\{u\}$ can be partitioned as

$$\{u\} = [\{u_s\}^{\mathrm{T}}, \{u_r\}^{\mathrm{T}}]^{\mathrm{T}}, \tag{28}$$

where $\{u_s\}$ and $\{u_r\}$ are the state vectors associated with the significant and the residual frequency subsystems respectively. The dynamic models of such subsystems are given by

$$\{\dot{u}_s\} = [A_s]\{u_s\} + [B_s]\{Q_s\}, \qquad \{v_s\} = [C_s]\{u_s\} \tag{29}$$

and

$$\{\dot{u}_r\} = [A_r]\{u_r\} + [B_r]\{Q_r\}, \qquad \{v_r\} = [C_r]\{u_r\}, \tag{30}$$

where equations (29) and (30) represent the dynamics of the significant and residual subsystems respectively. It is important to note that the residual interaction terms in equations (29) and (30) have been ignored, thus being treated as modelling error. The residual interactions may give rise to control and observation spillover, which may lead to instability [7]. Stability bounds as well as conditions to guarantee that residual interaction terms (spillover) do not lead to instability have been addressed early in the literature [33, 34].

In practice, the significant frequency subsystem refers to the show dynamics of the system, which normally spans the lower end of the frequency spectrum. Such a low-frequency subsystem accounts for most of the total kinetic energy of the system, while the residual dynamics represent only a very small or even negligible portion of the system's total energy. In practice, the measurements $\{v_s\}$ may be obtained through a set of narrowband-pass filters in order to get a clean measurement of the controlled modes without any contamination from the residual (high-frequency) subsystem. Accordingly, one can avoid the problem of the destabilization effect due to the measurement spillover from residual modes.

3. THE ACTIVE CONTROLLER

The structure of the active controller employed in this study is simply an output feedback control action. For the linear structural systems, the deterministic approach of regulating

a linear system may be invoked. Practical control implementations require that sensors and actuators be placed at certain accessible structural locations. Moreover, a minimum number of such control devices is apparently desired. If the output variables as well as control actions are measured at some specified nodal locations, then the state differential equation of the controlled subsystem can be rewritten as

$$\{\dot{u}_s\} = [A_s]\{u_s\} + [\bar{B}_s]\{F_s\} \quad \text{and} \quad \{v_s\} = [C_s]\{u_s\}, \tag{31}$$

where $[\tilde{B}_s] = [B_s][\Pi]$ and $[C_s] = [[0][\bar{C}_s]]$. The matrix $[\Pi]$ is a Boolean matrix that constructs the vector $\{F_s\}$ out of the full-order nodal force vector $\{Q_s\}$. The vector $\{F_s\}$ contains a selected set of non-zero entries that correspond to the actuators' locations. By examining the rank of controllability and observability matrices, one can simply conclude that the controllability and observability requirements for the system presented by equation (31) are satisfied if and only if each row of $[\tilde{B}_s]$ and each column of $[\bar{C}_s]$ have a non-zero entry. This conclusion is only true if the controlled modes are associated with unit-multiplicity eigenvalues. It is consequently concluded that the system can be made controllable and observable by using one sensor and one actuator, provided that they are located away from the nodes of the controlled modes. Now, one can consider a state-variable feedback control law of the form

$$\{F_s\} = -[G_c]\{u_s\}, \tag{32}$$

where $[G_c]$ is the controller gain matrix.

3.1. ESTIMATION OF THE SYSTEM STATES

The control law of equation (32) may not seem realistic in its present form, simply because the system states are not directly measurable. Actual direct measurements can only produce displacements and velocities of the structural points where sensors are attached. In this regard, a state estimator (observer) can be utilized to estimate the states of the controlled system [35]. That is, equation (32) is replaced by

$$\{F_s\} = -[G_c]\{\hat{u}_s\}, \tag{33}$$

where the control law is interconnected with the estimated state $\{\hat{u}_s\}$. Therefore, the observer is built using the same characteristics ($[A_s]$, $[\tilde{B}_s]$, $[C_s]$) of the controlled dynamics. The observer corrects its internal model by linear feedback of the error between the measured output $\{v_s\}$ and the estimated output $\{\hat{v}_s\}$. This can be written as

$$\{\dot{\hat{u}}_s\} = [A_s]\{\hat{u}_s\} + [\tilde{B}_s]\{F_s\} + [G_e][\{v_s\} - \{\hat{v}_s\}], \tag{34}$$

where $[G_e]$ is the estimator gain matrix, and $\{\hat{v}_s\} = [C_s]\{\hat{u}_s\}$. For the deterministic case, the state estimator can be designed as a Luneburger observer. If the system experiences state excitation noise as well as measurement for observation noise, then an optimal state estimator can be designed as a Kalman filter for the stochastic system.

If the error between the measured and estimated states is defined by

$$\{\varepsilon\} = \{u_s\} - \{\hat{u}_s\}, \tag{35}$$

then, utilizing equations (31) and (35), one can write the derivative of equation (35) in the form

$$\{\dot{\varepsilon}\} = ([A_s] - [G_e][C_s])\{\varepsilon\}. \tag{36}$$

For the linear time-invariant problem, the solution of equation (36) has the property that the error $\{\varepsilon\} \to 0$ as $t \to \infty$. Consequently, the asymptotic stability of the observer is determined by the behavior of the matrix $([A_s] - [G_e][C_s])$, whose characteristic values are the poles of the state estimator. By using pole allocation algorithms, such poles can be arbitrarily placed deep in the left half of the complex plane in order to achieve observer stability and the desirable fast convergence of the estimation error to zero [35]. Placing poles too far to the left-half plane, would result in large gain values $[G_e]$, thus causing the observer to become too sensitive to the observation noise. In general, a compromise can be achieved between the fast convergence and high sensitivity to measurement noise.

3.2. THE CONTROLLER GAIN MATRIX

The gain matrix $[G_c]$ of the control law of equation (33) can be determined by pole-placement algorithms. In fact, the closed-loop poles of the system can be located anywhere in the left-hand side of the complex plane. The closed-loop poles when placed very far to the left would result in the desired faster response in converging to the zero state. Such a fast response normally require large input amplitudes. In actual applications, input amplitudes must be bounded, where smaller values (i.e., smaller actuators) are always desired. To achieve this goal, a best compromise may be obtained by finding an optimal solution that satisfies certain performance criteria. In this regard, a quadratic integral criterion can be very useful in representing some physical quantities which are pertinent to the system's performance characteristics. In the structural vibrations, the objective is to suppress such vibration by minimizing the kinetic energy content in the excited modes. To this end, a performance index in terms of energy can be written as

$$\Gamma = \int_{t_0}^{t_f} \{u_s\}^{\mathrm{T}}[E]\{u_s\}\,\mathrm{d}t, \tag{37}$$

where the quadratic form of the controlled variable $\{u_s\}$ together with a properly chosen weighting matrix $[E]$ can be considered to represent the kinetic energy in the controlled modes. However, in order to penalize any excessive amplitudes of the control forces, the performance criterion of equation (37) can be modified to include the mean square input coverage as

$$\Gamma = \int_{t_0}^{t_f} [\{u_s\}^{\mathrm{T}}[E]\{u_s\} + \{F_s\}^{\mathrm{T}}[U]\{F_s\}]\,\mathrm{d}t, \tag{38}$$

where both the weighting matrices $[E]$ and $[U]$ are positive-definite symmetric matrices. For the linear structural system represented by equation (13), the weighting matrix $[E]$ is given by

$$[E] = \frac{1}{2}\begin{bmatrix} [I] & [0] \\ [0] & [M] \end{bmatrix}. \tag{39}$$

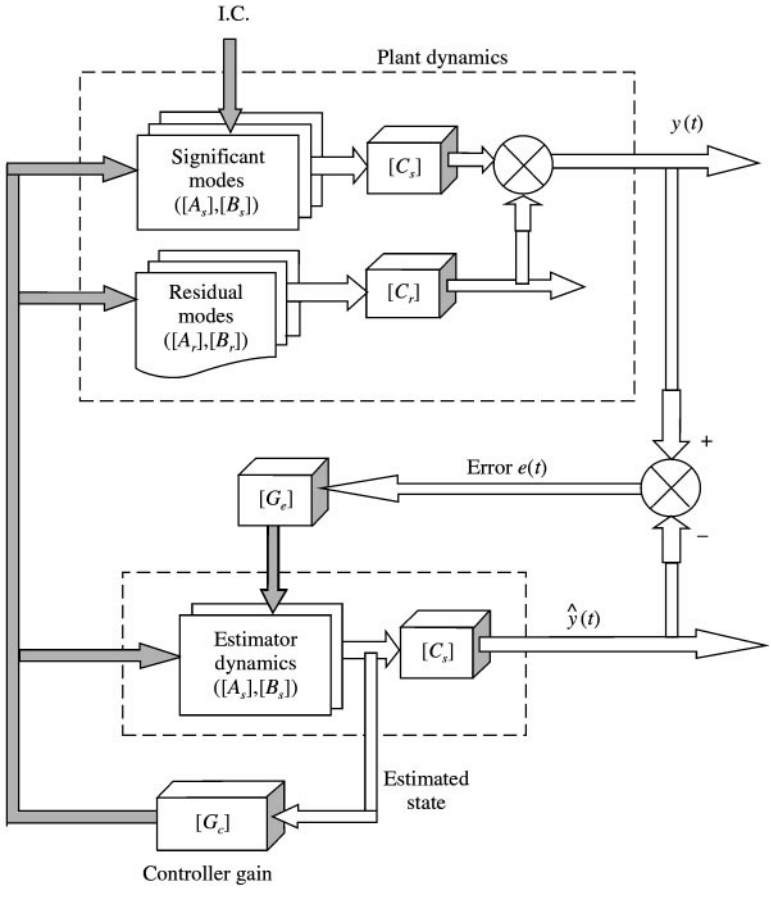

Figure 2. Flowchart of the active control scheme.

Now, the first quadratic term of equation (38) represents the kinetic energy content in the controlled modes. If the other weighting matrix for the input term is taken as identity matrix (i.e. $[U] = [I]$), then the second quadratic term of equation (38) represents the square of the control forces. Nevertheless, other appropriate values for $[U]$ can be selected.

The controller gain matrix $[G_c]$ can be determined by solving the steady state optimal regulator problem. In this case, the gain matrix is given by

$$[G_c] = -[U]^{-1}[\tilde{B}_s]^{\mathrm{T}}[P], \tag{40}$$

where $[P]$ is the solution of the following matrix algebraic equation of the Riccati type:

$$[A_s]^{\mathrm{T}}[P] + [P][A_s] - [P][\tilde{B}_s][U]^{-1}[\tilde{B}_s]^{\mathrm{T}}[P] + [E] = [0]. \tag{41}$$

When the system excitations and measurements are contaminated by noise, the stochastic separation principle can be applied. That is, the control gain matrix $[G_c]$ is obtained from the deterministic optimal control law, equation (33), with the performance index, equation (38), where the true state is replaced by the estimated state from the Kalman filter. The control law remains optimal in the sense it minimizes the expected value of the performance index. One must note that the dynamics of sensors and actuators are not included in the design of the controller. The flowchart of the complete active control scheme is shown in Figure 2.

TABLE 1

Frequencies of fixed–free beam

λ	$\eta = 0$	$\eta = 3$
1	3.515	4·6488
2	22·033	23·292
3	61·697	62·976
4	120·905	122·235
5	199·875	201·237
6	298·609	299·993
7	417·137	418·537
8	555·510	556·921
9	713·803	715·223
10	892·129	893·556

4. NUMERICAL SIMULATION

4.1. NUMERICAL EXAMPLE

An elastic beam of length 1 m which is fixed to a rotating rigid hub is considered. The beam geometric characteristics are represented by the geometric parameter $(EI/\rho AL)^{1/2} = 55{\cdot}2$. In this simulation, the beam is discretized by 12 equal finite beam elements. The corresponding frequency spectrum up to the 10th mode is displayed in Table 1, for non-rotating as well as rotating beams. In this case, the natural frequencies of the rotating beam are those for the in-plane (lead–lag) motion. Both the frequency and the speed of rotation are presented in the parametric forms; $\lambda = \omega/(EI/\rho AL)^{1/2}$ and $\eta = \Omega/(EI/\rho AL)^{1/2}$. The beam rotates at a constant angular speed of 1600 r.p.m., which is approximately equivalent to $\eta = 3$.

The dynamic model of the beam using the first six modes is considered as the plant dynamics. The active controller is implemented to control the dynamics of the first four modes, thus treating the remaining two modes (the fifth and sixth modes) as residual modes, equations (29) and (30). The active controller is represented by one sensor located at the tip point (node 13) and one actuator located at node 3, where the first four modes are controllable, as shown in Figure 3. In this configuration, modes 5 and 6 are subjected to both observation and control spillover. In order to aid in selecting the number of modes to be retained as the controlled dynamics, an energy index is introduced. The energy index $\mu_{\mathbb{E}}$ can be established as the ratio of the time average kinetic energy content $\langle \tilde{\mathbb{E}}_h^i \rangle_{\tau_1}$ in the high-frequency subsystem to the time-average kinetic energy content $\langle \tilde{\mathbb{E}}_l^i \rangle_{\tau_1}$ in the low-frequency subsystem as

$$\mu_{\mathbb{E}}^i = \langle \tilde{\mathbb{E}}_h^i \rangle_{\tau_1} / \langle \tilde{\mathbb{E}}_l^i \rangle_{\tau_1} = \left\langle \sum_{j=1}^{l_1-1} \tilde{\mathbb{E}}_j^i \right\rangle \Big/ \left\langle \sum_{j=l_1}^{l_2} \tilde{\mathbb{E}}_j^i \right\rangle, \tag{42}$$

where l_1 is the number of lower modes, l_2 is the total number of modes to be included in the dynamic model, and τ_1 is the time period of the lowest natural frequency. A very small value of $\mu_{\mathbb{E}}$ implies that the selected set of higher modes can be treated as residual modes.

Actuators used in rotating beams can be of the self-supporting generator type, like those developed in reference [4, 36]. Two control schemes are considered. The first controller

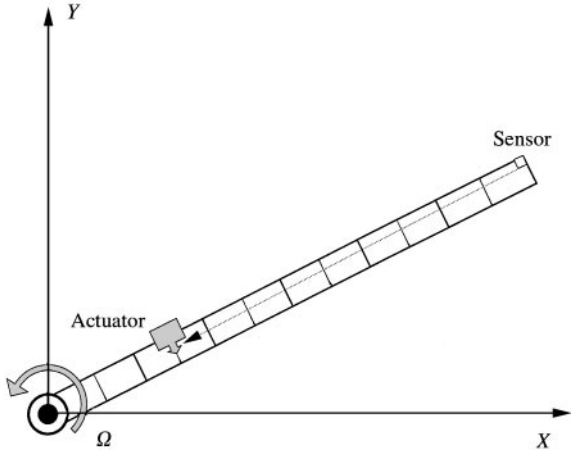

Figure 3. The active control configuration.

TABLE 2

The avtve controller gain matrices

Scheme 1		Scheme 2	
$[G_e]_{(8\times1)}$	$[G_c]^{\mathrm{T}}_{(8\times1)}$	$[G_e]_{(8\times1)}$	$[G_c]^{\mathrm{T}}_{(8\times1)}$
64·78	43·898	62·36	43·735
− 448·98	21·918	− 509·43	26·824
2008·62	34·080	2001·84	32·126
− 8317·52	38·723	− 8112·37	36·427
17·26	17·945	21·62	15·371
− 14·16	50·089	− 16·81	49·963
33·64	27·916	28·91	31·229
− 49·37	64·624	− 47·22	58·026

(*scheme* 1) is designed based on an elastodynamic model of a rotating beam, while the second controller (*scheme* 2) is derived for a non-rotating elastic beam. In the second scheme, the observer model and the optimal control law are based on the following simplified form of equation (12):

$$[M\{\ddot{e}\} + [K_e]\{e\} = \{Q_e\}. \tag{43}$$

In either case, the matrices $[\bar{B}_s]_{(8\times1)}$ and $[\bar{C}_s]_{(1\times8)}$ contain only the non-zero entries that are associated with the first four modes, which are evaluated at the corresponding actuator and sensor locations respectively.

The state estimator, as described by equation (34), is established. For *scheme* 1 the estimator has an internal model of the first four modes of a rotating elastic beam. The estimator gain matrix $[G_e]_{(8\times1)}$ is computed for the completely observable system $([A_s], [C_s])$ by using a pole-allocation algorithm, where the error between measurements and computations is forced to die out at an exponential rate of e^{-10t}. That is, the spectrum of $([A_s] - [G_e][C_s])$ lies to the left of a vertical line passing through $(-10, 0)$ on the real axis of complex plane. The gain values are presented in Table 2.

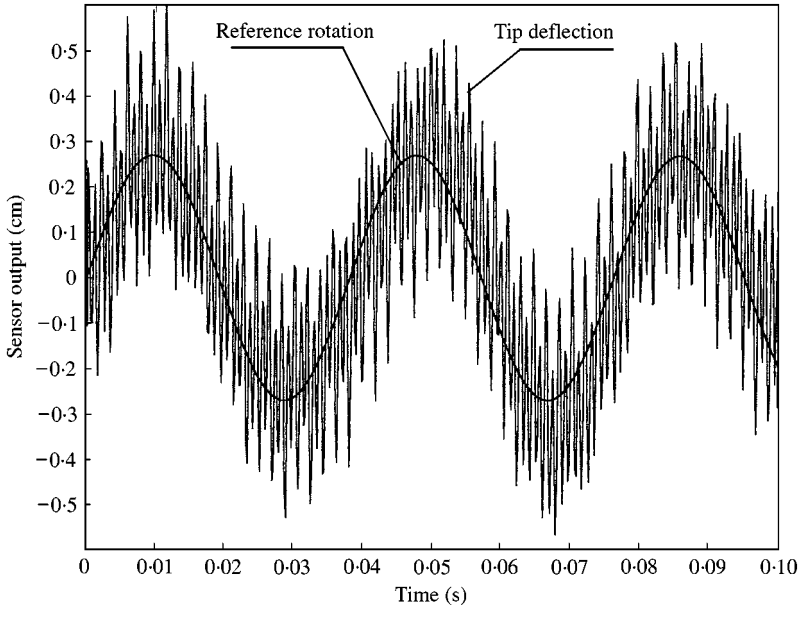

Figure 4. The undamped tip point response.

The controller gain $[G_c]_{(1\times 8)}$ is obtained for the steady state optimal regulator problem by solving the algebraic matrix equation of the Riccati type, as given by equation (41). The optimal control law is invoked to minimize the performance index of equation (38). In this example, the weighting matrix $[U]$ is set equal to $\frac{1}{2}[I]$. The controller gain matrix is computed and presented in Table 2. Similar computations are performed to obtain observer and controller gain matrices for *scheme* 2.

The undamped vibrational response of the tip point of the beam without control, as represented by the sensor output, is shown in Figure 4, where the elastic degrees of freedom are represented by the first six modal co-ordinates. In Figure 5, the effect of material damping (2% modal damping in all modes) is present. The dynamic response of the tip point after the application of the active controller (*scheme* 1) is shown in Figure 6.

The total kinetic energy in the vibrational modes can be expressed in terms of a normalized energy parameter [37]. The energy parameter $\hat{\mathfrak{R}}_j$ represents the ratio of the unweighted energy in the jth damped mode to the unweighted energy of the same undamped mode. This can be written for the significant (controlled) and the residual mode subsystems, respectively, as

$$\hat{\mathfrak{R}}_s = \sum_{j=1}^{(m-k)} (\omega_j^2 u_j^2 + \dot{u}_j^2)/\omega_j^2, \qquad \hat{\mathfrak{R}}_r = \sum_{j=(m-k)}^{m} (\omega_j^2 u_j^2 + \dot{u}_j^2)/\omega_j^2, \tag{44, 45}$$

where m is the total number of modes that represent the dynamics of a plant, and k is the number of modes in the high-frequency subsystem (residual modes). These are calculated and presented in Figures 7 and 8. In order to show the effect of the small amount of material damping (2% modal damping) on stabilizing the residual modes, the energy parameter for the residual modes without material damping is calculated and displayed in Figure 9. The figure shows that the active controller tend to destabilize the uncontrolled residual modes. However, the small amount of the natural material damping is sufficient to stabilize such modes, as shown in Figure 8.

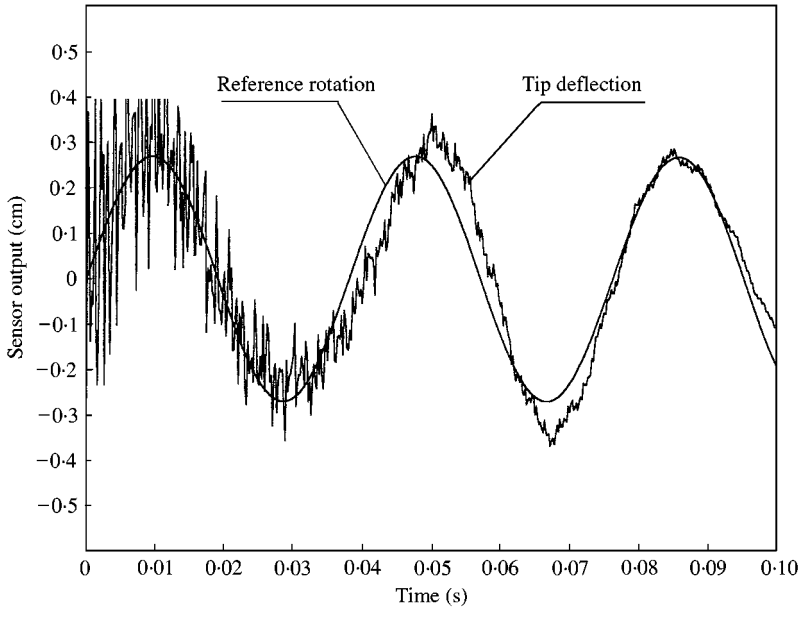

Figure 5. The tip point response with material damping.

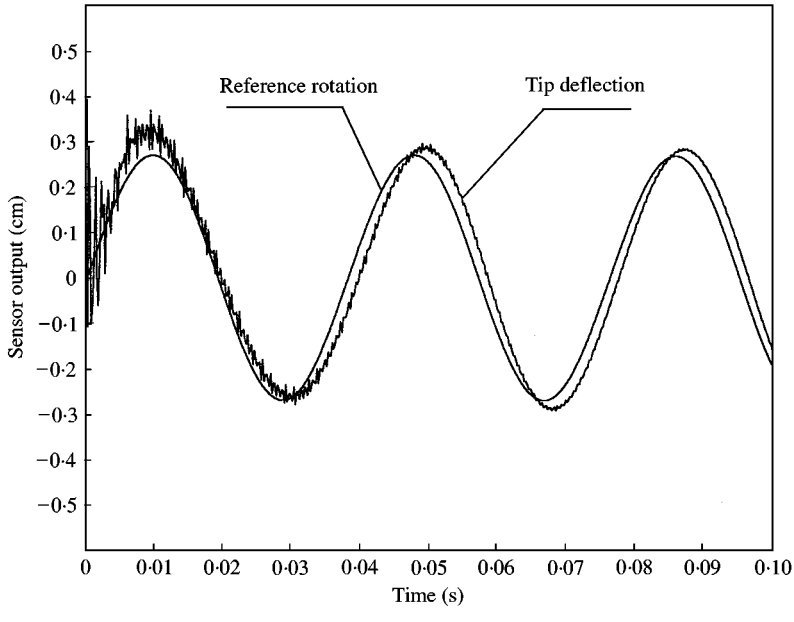

Figure 6. The tip point response with control.

The other controller (*scheme* 2) is considered, and the corresponding controller gain matrix is calculated and presented in Table 2. The simulation results show that the controller performance has deviated from the optimal behavior of *scheme* 1, as displayed in Figure 10. Figures 11 and 12 show comparisons of the estimator errors and the actuator forces respectively for the two control schemes.

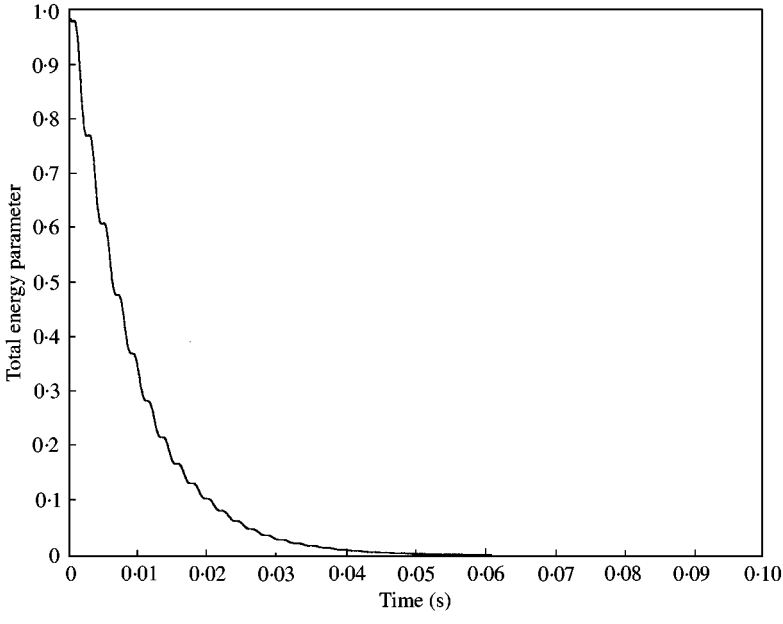

Figure 7. Energy in the controlled modes.

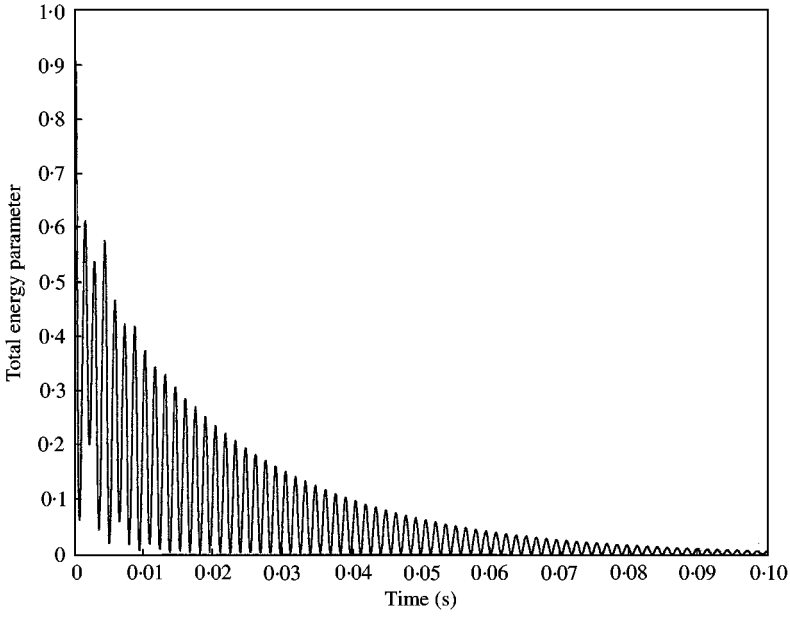

Figure 8. Energy in the residual modes.

5. CONCLUSION

A theoretical investigation into the application of active vibration control to rotating beams is presented. The rotating beam is modelled by using the finite element approach.

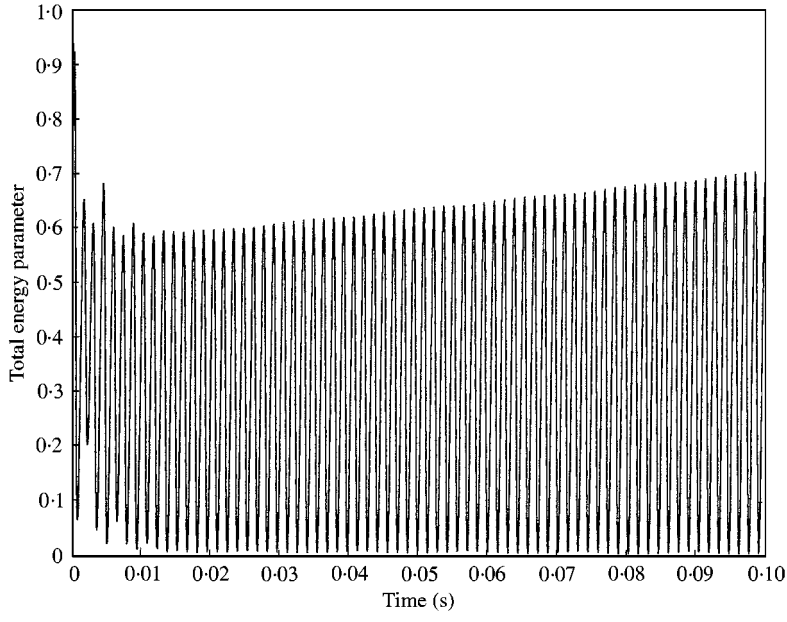

Figure 9. Energy in the residual modes without material damping.

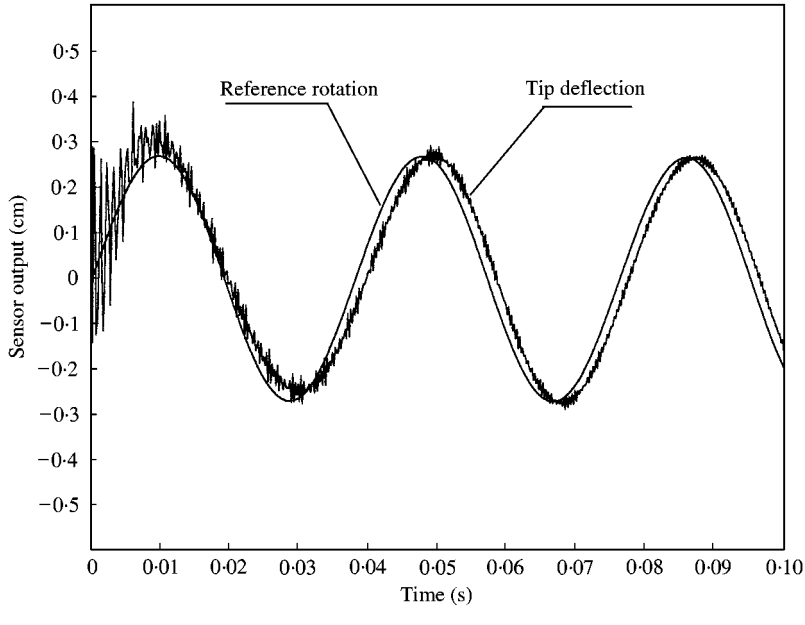

Figure 10. The tip point response with control (*scheme* 2), - - -, reference motion of tip point.

The problem of vibration suppression in rotating elastic beams is formulated by using active control techniques. A computational algorithm is established to generate numerically the finite element model as well as the calculation of the gain matrices of both the state estimator and the optimal controller. In practical applications, the plant dynamics, as

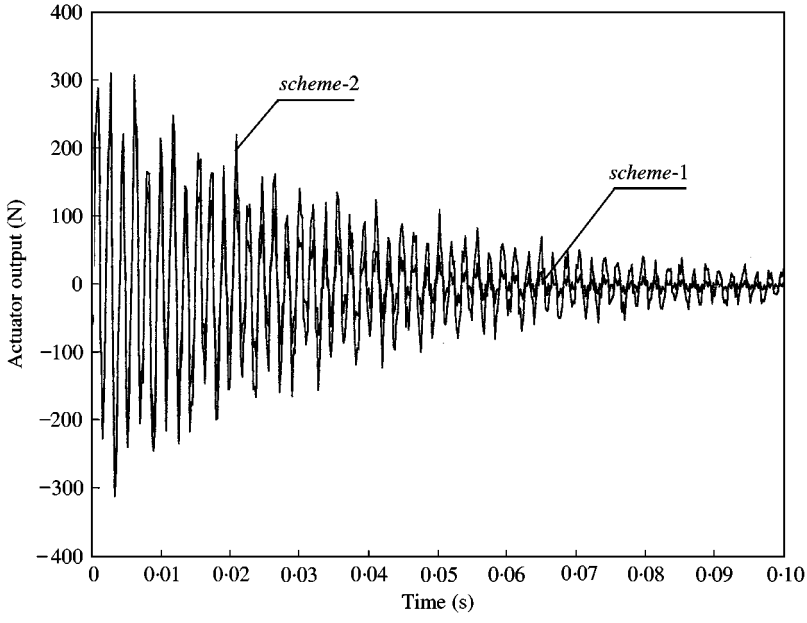

Figure 11. The actuator output: —, *scheme* 1; - - -, *scheme* 2.

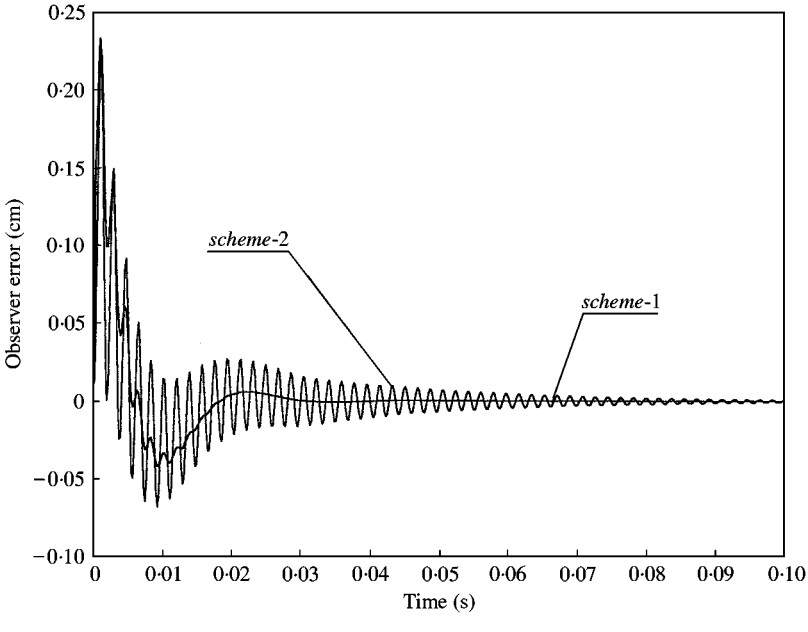

Figure 12. The observer error: —, *scheme* 1; - - -, *scheme* 2.

shown in Figure 2, is replaced by the actual physical structure. The estimator dynamics is represented by a reduced order modal form of the finite element mathematical model. Either analytically calculated or experimentally determined mode shapes can be used as a basis for the modal transformation. For real-time control, vibration measurements are

obtained by a set of sensors (e.g., displacement transducers with spectral filters), and fed to the controller, which can be programmed on an on-board microprocessor.

It is noteworthy to emphasize the importance of including the effect of rotation in the derivation of the controller equations. The numerical results of the two schemes presented show that ignoring the effect of rotation in controller design may result in inaccurate gain values that will eventually result in poor performance, and may lead to instability at higher rates of rotation.

The numerical simulation reveals the potential of the numerical scheme developed in analysis and design of such control systems, by considering different controller arrangements. The effect of material damping on the stability of the residual modes can also be easily addressed.

ACKNOWLEDGMENTS

The support of King Fahd University of Petroleum & Minerals is greatly appreciated.

REFERENCES

1. M. CROSBY and D. KARNOPP 1973 *The Shock and Vibration Bulletin* **43**, 119–133. The active damper—a new concept for shock and vibration control.
2. M. COTTEREL 1975 *Stress, Vibration and Noise Analysis in Vehicles. New York: Halsted Press*, p. 253–281. Theoretical analysis of an active suspension fitted to a London buss.
3. Y. A. KHULIEF and S. P. SUN 1989 *American Society of Mechanical Engineers Journal of Dynamic Systems, Measurements and control*, **111**, 521–527. Finite element modeling and semi-active control of vibrations in road vehicles.
4. L. WALKER and P. YANESKE 1976 *Journal of Sound and Vibrations* **46**, 157–176. Characteristics of an active feedback system for the control of plate vibrations.
5. P. A. NELSON and S. J. ELLIOTT 1992 *Active Control of Sound*. New York: Academic Press.
6. M. J. BALAS 1978 *SIAM Journal of Control and Optimization* **16**, 450–462. Modal control of certain flexible dynamic systems.
7. M. J. BALAS 1978 *IEEE Transactions on Automatic Control* **AC-23**, 673–679. Feedback control of flexible systems.
8. L. MEIROVITCH and H. OZ 1980 *Journal of Guidance and Control* **3**, 569–577. Modal-space control of large flexible spacecraft possessing ignorable coordinates.
9. C. R. FULLER, G. P. GIBBS and R. J. SILCOX 1990 *International Congress on Recent Developments in Air and Structure-Borne Sound and Vibration, Auburn University, AL, U.S.A.* 657–662. Simultaneous active control of flexural and extensional power flow in beams.
10. R. L. CLARK, J. PAN and C. H. HANSON 1992 *Journal of Acoustical Society of America* **92**, 871–876. An experimental study on the active control of multiple wave types in an elastic beam.
11. J. F. BLOCK and T. W. STRGANAC 1988 *American Institute of Aeronautics and Astronautics Journal of Guidance, Control and Dynamics* **21**, 838–854. Active control for a nonlinear aeroelastic structure.
12. M. J. BERNNAN, M. J. DAY and R. J. RANDALL 1998 *American Society of Mechanical Engineers Journal of Vibration and Acoustics* **120**, 1–12. An experimental investigation into the semi-active and active control of longitudinal vibrations in large tie–rod structure.
13. G. R. SKIDMORE and W. L. HALLAUER 1985 *Journal of Sound and Vibration* **101**, 149–160. Modal space active damping of a beam-cable structure: theory and experiment.
14. T. BAILEY and J. E. HUBBARD 1985 *Journal of Guidance and Control* **8**, 605–611. Distributed piezo-electric polymer active vibration control of a cantilever beam.
15. S. DUKE and J. E. HUBBARD 1988 *Automatica* **24**, 619–627. Distributed actuator control design for flexible beams.
16. R. SETOLA 1998 *Journal of Sound and Vibration* **213**, 777–790. A spline-based state reconstructor for active vibration control of a flexible beam.

17. R. STANWAY and C. R. BURROWS 1981 *American Society of Mechanical Engineers Journal of Dynamic Systems Measurement and Control* **103**, 383–388. Active vibration control of a flexible rotor on flexibly-mounted journal bearings.
18. S. M. YANG and G. J. SHEU 1999 *American Society of Mechanical Engineers Journal of Applied Mechanics* **66**, 254–259. Vibration control of a rotating shaft: an analytical solution.
19. R. F. FUNG and K. W. CHEN 1998 *Journal of Sound and Vibration* **214**, 605–637. Dynamic analysis and vibration control of a flexible slider-crank mechanism using PM synchronous servo motor drive.
20. A. ANKARALI and H. DIKEN 1997 *Journal of Sound and Vibration* **204**, 162–170. Vibration control of an elastic manipulator link.
21. W. BERNZEN 1999 *Journal of Intelligent Robotic Systems*: *Theory and Applications* **24**, 69–88. Active vibration control of flexible robots using virtual spring damper systems.
22. P. LIKENS, F. BARBERA and V. BADDELEY 1972 *American Institute of Aeronautics and Astronautics Journal* **11**, 1251–1258. Mathematical modeling of spinning elastic bodies for modal analysis.
23. Y. A. KHULIEF 1989 *Journal of Sound and Vibration* **134**, 87–97. Vibration frequencies of a rotating tapered beam with end mass.
24. B. J. LAZAN 1968 *Damping of Materials and Members in Structural Mechanics*. Oxford: Pergamon Press.
25. F. STURLA and A. ARGENTO 1996 *American Society of Mechanical Engineers Journal of Vibration and Acoustics* **118**, 463–468. Free and forced vibrations of a spinning viscoelastic beam.
26. E. R. MARSH and L. C. HALE 1998 *American Society of Mechanical Engineers Journal of Vibration and Acoustics* **120**, 188–193. Damping of flexural waves with imbedded viscoelastic materials.
27. P. W. LIKINS 1967 *American Institute of Aeronautics and Astronautics Journal* **5**, 1304–1308. Modal methods for analysis of free rotations of spacecraft.
28. A. A. SHABANA and R. WEHAGE 1983 *American Society of Mechanical Engineers Journal of Mechanisms, Transmission and Automation in Design* **105**, 370–378. Variable degree of freedom component mode analysis of inertia variant flexible mechanical systems.
29. T. J. SPANOS and W. S. TSUHA 1991 *Journal of Guidance* **14**, 260–267. Selection of component modes for flexible multibody simulations.
30. Y. A. KHULIEF 1997 *Journal of Computer Methods In Applied Mechanics and Engineering* **26**, 41–55. On the finite element dynamic analysis of flexible mechanisms.
31. L. MEIROVITCH 1974 *American Institute of Aeronautics and Astronautics Journal* **12**, 1337–1342. A new method of solution of the eigenvalue problem for gyroscopic systems.
32. Y. A. KHULIEF and M. A. MOHIUDDIN 1992 *Journal of Finite Elements in Analysis and Design* **97**, 23–31. On the dynamics of rotors using modal reduction.
33. D. D. SILJAK 1976 *Automatica* **12**, 309–320. Multilevel stabilization of large scale systems: a spinning flexible spacecraft.
34. R. IWENS, R. BENHABIB and R. JACKSON 1980 *Joint Automatic Control Conference, San Francisco, CA*. A unified approach to the design of LSS control systems.
35. H. KWAKERNAAK and R. SIVAN 1972 *Linear Optimal Control Systems*. New York: John Wiley and Sons, Inc.
36. R. A. BURDISSO and J. D. HEILMANN 1998 *Journal of Sound and Vibration* **214**, 817–831. A new dual-reaction mass dynamic vibration absorber actuator for active vibration control.
37. Y. A. KHULIEF 1980 *M.Sc Thesis, The Hatfield Polytechnic (University of Hertfordshire), Hatfield, England*. Active control of vibrations in mechanically flexible systems.